

Assessing Heat Treatment Distortion Sensitivity

A. M. Freborg, Z. Li, and B. L. Ferguson

Deformation Control Technology Inc., Cleveland, Ohio, USA

Abstract

Distortion has been cited as a primary problem for all heat treaters in many surveys of the industry, and remains a primary concern. Consequently, metallurgical and manufacturing engineers continue to face the challenge of minimizing part distortion through the prudent application of process controls during the various steps in the heat treatment process. Such process engineering requires foundational understanding of process variation relative to corresponding variation in part response. This study reports on the use of a simple coupon shape to assess sensitivity of a steel alloy during quenching in terms of its residual stress and distortion responses. Using a rectangular test bar that has a series of notches machined on one face, a series of carburization and quench hardening trials were conducted. Local distortion was measured along the length of the bar, as well as residual stress using both X-RAY diffraction and Barkhausen noise methods. The analyses were supplemented by use of heat treatment modeling to study the interaction of thermal and transformation strains on resulting distortion and residual stress in the coupons. The data were finally differentiated by the quenching process conditions. This permitted process sensitivity analyses linking local dimensional and measured residual stress changes to the method and consistency of the quench practice. The procedure demonstrates the utility of using a simple steel coupon in a standardized procedure for heat treatment process assessment.

Introduction

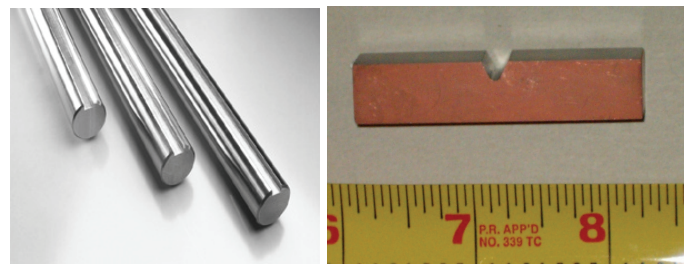
Heat treatment of steel is accomplished through application of controlled heating and cooling to drive solid-state modification of the steel's metallurgical structure. In quench hardening, the typical structural changes involve transformation from a face centered cubic (fcc) austenitic structure and high temperature to body centered tetragonal (bct) martensitic or mixed body centered cubic (bcc) bainitic/pearlitic structures. Variations in steel alloy content, cooling rates and part geometry all contribute to potential variation in heat treatment response – some desired (e.g. alloy or cooling adjustment to facilitate greater hardening response), and others not (e.g. non-uniform quench application causing localized variation in properties or distortion).

Accompanying these metallurgical modifications are dimensional and residual stress changes driven by volumetric expansion and contraction of the steel microstructure. Again

such changes may be desirable (e.g. residual compression to improve fatigue life) or detrimental (e.g. excessive dimensional change or cracking from residual tension).

One of the principle responsibilities for the heat treating engineer is management and control of the processes affecting these responses in the steel. Such engineering is typically accomplished through application of experience, prototyping, and production trials. As typical production parts may contain differing geometric features and be made from different steel alloys, the complexity of heat treatment analysis can greatly expand. Recently, more analytical engineering techniques such as simulation and modeling have also begun to be used for heat treatment to help address these complexities. [1-4]

For many complex steel parts such as gears and shafts, important process sensitivity data can be obtained through process trials using combinations of more simple shapes. Physical testing and process modeling of these shapes have been shown to provide sound data for direct application to process control in the more complex corresponding part. For example, both keyed shafts and notched bars have been used in process control work to characterize distortion and residual stress response in quenching. (cf. Figure 1). [5-7]



a) Keyed shafts

b) Notched bar (copper plated for carburization masking)

Figure 1: a) Keyed shafts; and b) notched-bars used in heat treatment process analyses.

As part of a larger project to improve helicopter transmission gear fatigue performance for the US Army rotorcraft fleet, DCT is currently investigating the multiple effects of heat treatment, shot peening, laser shock peening and cavitation peening on residual stress in Pyrowear 53 steel. With the large number of process variables, volume of required testing, and high cost of this aerospace steel it was imperative to develop a small and relatively simple test coupon for the initial process assessments. This paper will focus on the heat

treatment aspect of this work, and describe how a simple coupon shape was used to assess the sensitivity of carburized Pyrowear 53 steel in two different quenching operations. Heat treatment process sensitivity was characterized in terms of residual stress, distortion response, and Barkhausen noise. Process modeling was then validated against the coupon physical data, permitting future use of the model in additional process variation studies.

Test Coupons

To begin the process sensitivity study required for the helicopter transmission gears, DCT developed a triple-notched bar design to help characterize the effects of multiple notched geometries and carburized surfaces typically encountered in these parts. A schematic of the triple-notch bar design is shown in Figure 2.

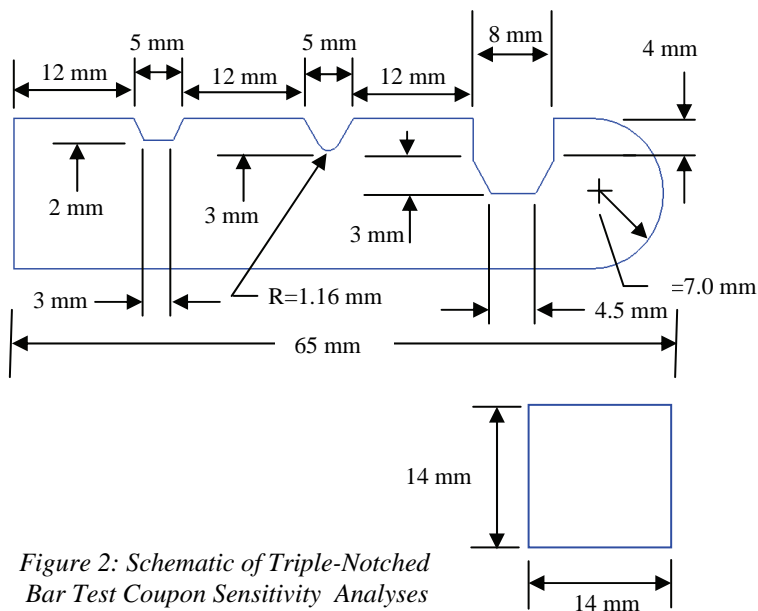


Figure 2: Schematic of Triple-Notched Bar Test Coupon Sensitivity Analyses

As used in rotorcraft transmission gears, Pyrowear 53 is subjected to a six (6) step heat treating practice involving case carburizing, quench hardening, deep freezing, and a double temper. This processing sequence is summarized in Table 1.

Table 1: Heat Treat Process Routing used for Pyrowear 53 Transmission Gears

Steps	1	2	3	4	5	6
Heat Treat	Case Carburize	Stress Relief	Aust & Quench	Deep Freeze	1 st Temper	2 nd Temper

For the sensitivity analysis, six (6) specimens were first machined, and then directionally carburized on the notched side only and around of the bar end radius to a depth of 0.040”.

Following this step the samples were solution annealed before being separated into two groups for the quenching sensitivity analysis. A photograph of a machined sample, copper masked prior to carburization, is shown in Figure 3.



Figure 3: Machined Test Coupon Prior to Heat Treatment, showing Copper Masking for directional Carburization

Heat Treatment

For the process sensitivity testing, three (3) of the notched samples were processed via the convention route using a 150°F oil quench, and three (3) specimens were processed using an alternative intensive quenching procedure in which water flow as directed at 14 m/sec within a specialized fixture directly onto the notched face. The quenching fixture for the intensive quench is shown in Figure 4.



Figure 4: Triple Notched Test Bar in Intensive Quenching Heat Treating Fixture

With the required fixture, the intensive quench operation was performed individually on each of the three specimens designated in the test matrix. The oil quench was performed as a batch operation, with all three of its designated specimens quenched together in a basket. Following their respective quench operations, all of the samples were again processed together in a -100°F deep freeze to remove retained austenite, and then received a final double tempering at 450°F.

Testing and Sensitivity Analysis

In heat treated steel parts, several quantitative measures of heat treating response include hardness, dimensional change and residual stress. It is these attributes which were comparatively examined in the six notched and heat treated samples.

The processing and testing of the notched specimens was augmented by heat treatment simulation using the DANTE[®] computer model. The carburizing, quenching, deep freeze and double temper were simulated in a 3-D finite element model of the notched bar for both oil and intensive quenching process routes. Comparison of the predicted heat treatment response from the simulation with the actual results from multiple samples was then used as an additional gage of process sensitivity.

Sample Reference Positions

Using the triple-notched bar shown in Figures 2 and 3 as a standard for the sensitivity analysis, surface reference positions were designated for the flat regions adjacent to the notches. Additionally, the zero reference for deflection was defined as the line connecting both surface endpoints along the notched side of the sample. The reference positions and deflection reference line for the distortion measurements are shown in Figure 5.

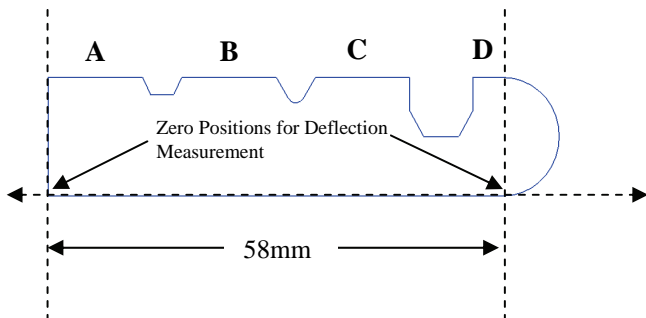


Figure 5: Surface Location Reference Positions for Surface and Deflection Measurements in the Heat Treated, Triple-Notched-Bar

Carburized Layer

The base carbon of Pyrowear 53 is 0.10%. For the sensitivity analysis, each sample was selectively carburized on the notched face and around the radial end to an effective case depth of 0.040". The heat treatment simulation provides an informative means of visualizing the carburized layer. Figure 6 shows a contour map of the carbon profile through the bar cross section. Simulation accuracy has been verified in a number of prior studies with the Pyrowear 53 material. [8]

Hardness

Hardness is often used as an indicator of sound and uniform heat treatment. As an initial measure of variability and

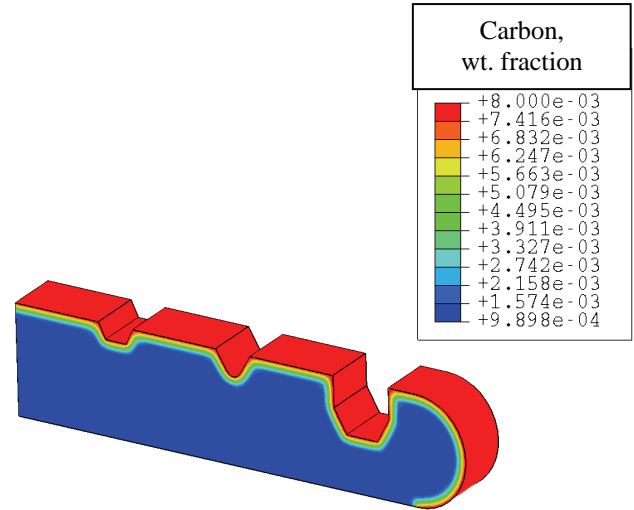


Figure 6: Simulation Predicted Carbon Profile (0.040" Case) through Sample Cross Section

sensitivity, hardness was measured on the carburized flat surfaces adjacent to the notches. Measured hardness at the four reference positions (cf. Figure 5) for each of the six samples is summarized in Table 2.

Table 2: Surface Hardness Comparison for the Six Heat Treated Samples, Including Predicted Hardness from Simulation

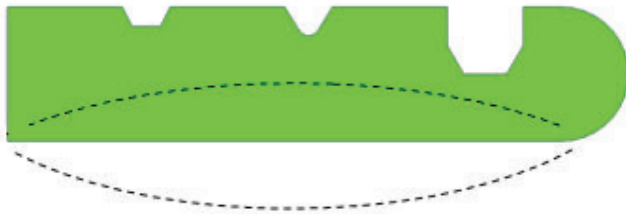
SAMPLE	CONDITION	HARDNESS (HRC) AT POSITION			
		A	B	C	D
1	Int. Quench	59	60	60	59.5
2	Int. Quench	59	60	60	58
3	Int. Quench	60	61	61	60
4	Oil Quench	59.5	61	61	60.5
5	Oil Quench	60	61	61	61
6	Oil Quench	61	61.5	61	61.5
MODEL IQ	Sim. IQ	58.0	58.0	58.0	58.0
MODEL OIL	Sim. Oil	57.8	57.8	57.8	57.8

The data show the respective hardness measurements to vary within within +/- 1 HRC for both processes across all samples and positions. Also, the hardness for the oil quenched samples is on average 1 HRC higher than in the IQ samples. Interestingly, the simulation predicts the opposite scenario, though in the simulation the overall hardness is underpredicted by 1.5 HRC. These variations are however minor. Based on the hardness measurements alone, one cannot make any diffinitive comparison with respect to process sensitivity and corresponding material response

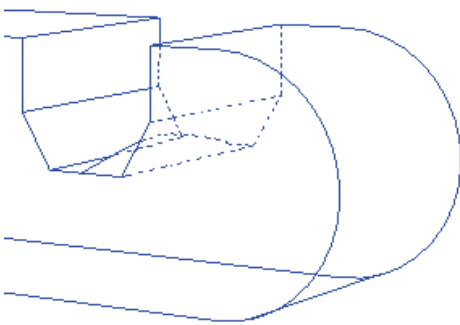
Distortion

With three notches of varied dimensions and an associated carburized case on a single side, the notched bar should be particularly sensitive to localized distortion. During quench hardening, size and shape changes in the steel occur due to non-uniform thermal expansion and contraction, as well as volumetric changes in the crystal structure due to phase changes.[9] For example, during quenching the face centered cubic structure of austenite typically transforms to martensitic, bainitic or mixed ferritic structures. These transformations are accompanied by a corresponding volumetric expansion which acts counter to the thermal contraction. For steels with complex shapes the associated thermal gradients introduce non-uniformities in transformation which can result in part distortion. Additionally, chemistry variation in the steel (e.g. from a carburized case or alloy segregation) also produces variation in the phase transformations occurring during quenching. Like thermal gradients, the phase transformation variation from chemical gradients can also produce non-uniform dimensional response during heat treating. [10] By introducing a controlled and repeatable thermal and chemical variation in a test coupon, variation in test coupon dimensional change can be used as one measure of process sensitivity.

For the triple notched-bar in this study, two primary measures of distortion were quantified: 1) Bow of the bottom surface along the axial direction; and 2) Bulge along the transverse direction on the bottom surface of the large notch. These measures are illustrated schematically in Figure 7.



a) Specimen Bow along Axial Direction

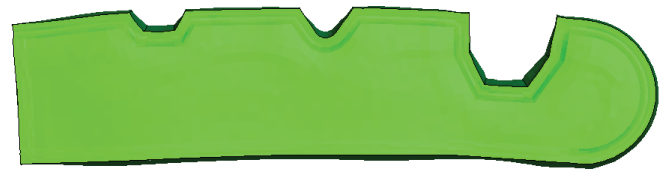


b) Bulge on Bottom Surface of Large Notch

Figure 7: Schematic Illustration of Distortion Metrics used in the Heat Treat Sensitivity Analysis of the Triple Notched-Bar

The distortion response of the carburized, notched sample to heat treatment showed a marked difference between the oil and intensive quenching processes that was not reflected in the hardness measurements. This difference correlated directly with the distortion predictions obtained from the DANTE heat treatment model. A laser light profilometer was used to gage the distortion in the physical specimens along the bottom and large notch surfaces. This data was then compared with the results predicted by simulation. Since each of the six samples was independently tested with the profilometer, this provided an additional measure of process variability for each quench practice.

A general comparison between the observed distortion response for the two quench practices is shown in Figure 8. The figures illustrate a 10X magnified view of the general distortion response seen in the physical samples and predicted by the simulations. For the oil quench process, the bars bowed upward in the direction of the notches. The intensively quenched bars bowed in the opposite direction.



a) Oil Quenched Specimen



b) Intensively Quenched Specimen

Figure 8: Distortion Response for the Notched Bars as seen in the Physical Samples and Predicted by the Heat Treatment Computer Model. Distortion magnified 10X.

Additionally, one can see a bulge in the bottom of the large notch for both processes. Physically present in the physical samples after heat treatment, this bulge was also predicted by the DANTE models.

Use of the laser profilometer enables a quantitative assessment of the distortion response, both in terms of variation between processes as well as from sample to sample for the same process. Figure 9 shows a comparison of the predicted to measured bottom surface deflections for all of the specimens. As predicted in the DANTE models, the intensively quenched samples all bowed downward (shown as a '-' displacement in the plot), while the oil quenched samples bowed upwards ('+' displacement in the plot). For the intensive quenched simulation, the prediction varied between 0 to +10 μ m of the

measured values. For the oil quench, the direction and general magnitude of the distortion was correctly predicted, the simulation had a wider variation (0 to +25 μm). This is likely due to application of an over estimated heat transfer coefficient in the oil model, as well as the fact that the oil quench was a batch practice with greater inherent heat transfer variability in the process itself. Such variation is more clearly evident when examining the processes individually.

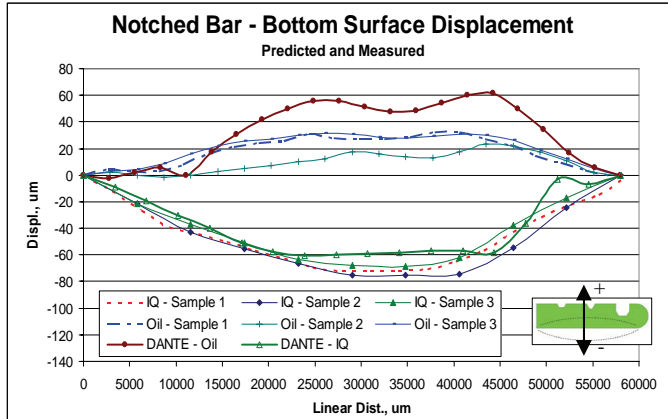


Figure 9: Comparison of Predicted and Measured Distortion (Bow) along Length of Sample Bottom Surface.

For the batch oil quench, samples #4 and 6 showed strong consistency in the magnitude of measured distortion (cf. Figure 10). Measured distortion between these specimens varied to within $\pm 5.0\mu\text{m}$. Sample #5 however showed marked variation, differing in bowing by as much as $20\mu\text{m}$.

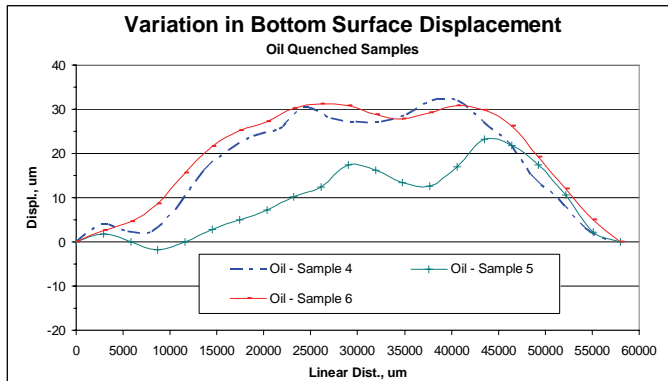


Figure 10: Measured Variation in Bottom Surface Displacement for the Oil Quenched Specimens.

For the three intensively quenched specimens, bar-to-bar consistency was improved to ± 8 to $10\mu\text{m}$. The magnitude of the bow however was about $2.3\times$ greater, and occurred in the opposite direction (cf. Figures 10 and 11).

The bar-to-bar consistency for each process indicates greater heat transfer inconsistency in the batch process. And while all

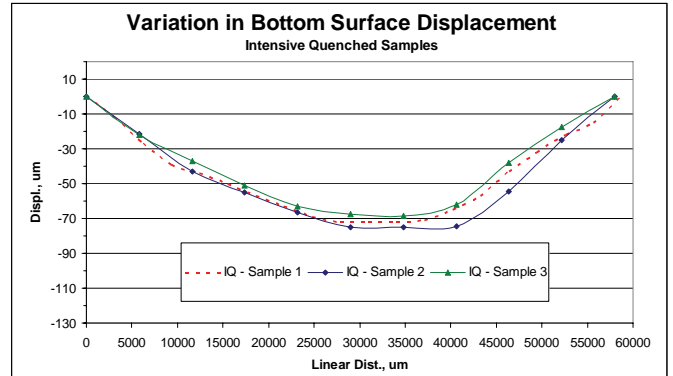


Figure 11: Measured Variation in Bottom Surface Displacement for the Intensive Quenched Specimens.

samples showed essentially the same hardness, timing and sequence of the martensitic phase transformation as clearly different for the two quench processes. This is evident from the markedly differing bowing behavior, and should be reflected in the internal residual stresses.

Another distortion metric investigated for this sample was the bulge in the bottom of the large notch (see Figure 7b). Both samples exhibited a central bulge on the notch bottom, which was also predicted by the DANTE heat treatment simulation. The measured and predicted bulge for each specimen and the two models are summarized in Table 3. The data indicate a greater amount of bulge for the intensive quenched samples, indicative of the sharp thermal gradient in the notch during the initial stages of the intensive quench. Figure 12 shows comparative contour plots of the notch bulge for the two processes, and provides a clear view of the bulge morphology. The predicted bulge was within 0.001mm to 0.003mm of the measured values.

Table 3: Measured and Predicted Bulge on the Bottom Surface on the Large Notch

SAMPLE	PROCESS	BULGE, mm
1	Int. Quench	0.060mm
2	Int. Quench	0.070mm
3	Int. Quench	0.060mm
4	Oil Quench	0.040mm
5	Oil Quench	0.060mm
6	Oil Quench	0.045mm
IQ Model	Int. Quench	0.057mm
Oil Model	Oil Quench	0.039mm

Additional insight into the differences in observed distortion behavior was obtained through assessment of the third sensitivity attribute -- residual stress.

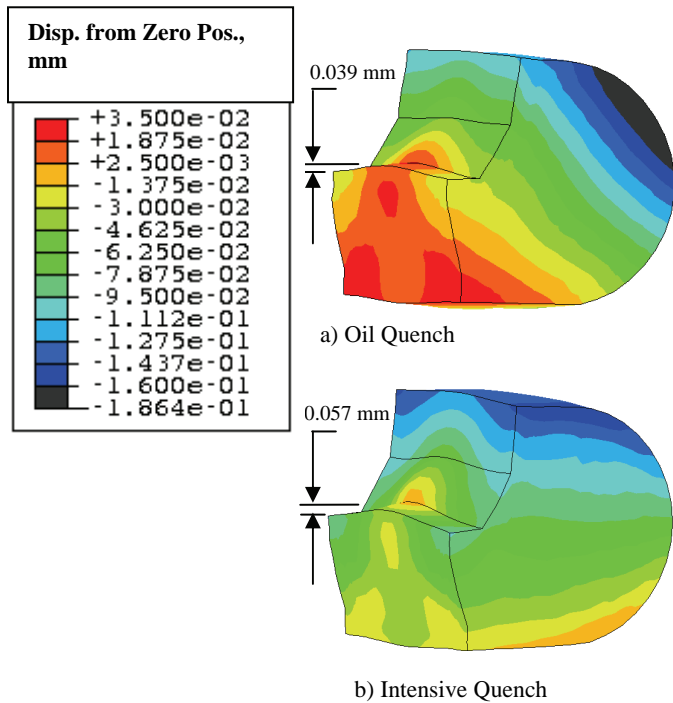


Figure 12: Comparison of Simulation Predicted Bulging in the Bottom of the Large Notch for the Oil and Intensive Quenched Specimens (Mag. 10X).

Residual Stress

The thermal and transformation strains from heat treatment may also impart residual stresses into the steel. Coupled with the predicted and observed distortion, the residual stress variations can provide another measure of material process sensitivity.

Surface residual stresses were calculated from X-RAY diffraction measurements (XRD) for surfaces A, B, C and D (cf. Figure 5) for each of the six heat treated test pieces. Measurements were obtained using an LXR D goniometer (cf. Figure 13) at Proto Mfg. Ltd. The comparative stress values are given in Table 4.

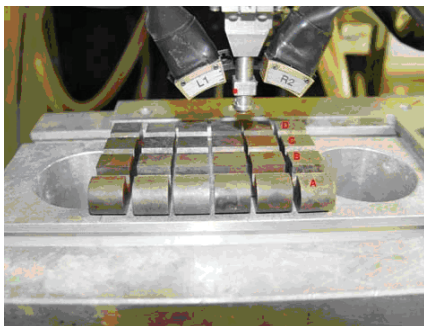


Figure 13: LXR D Goniometer with Carburized Triple Notched Bars for Surface X-RAY Testing of Heat Treatment induced Residual Stress. Photo courtesy of Proto Mfg. Ltd.

Table 4: Measured and Predicted Surface Residual Stress (Axial) at Four Reference Locations on the Sensitivity Specimens

SAMPLE	PROCESS	RESIDUAL STRESS (ksi); SURFACE LOCATION ¹			
		A	B	C	D
1	IQ	-74	-85	-58	-74
2	IQ	-72	-88	-75	-81
3	IQ	-68	-82	-56	-74
4	OQ	-19	-33	-25	-26
5	OQ	-21	-22	-24	-23
6	OQ	-18	-22	-23	-21
Model IQ ²	IQ	-84.1	-84.5	-84.8	-80.9
Model Oil ²	OQ	-39.8	-34.5	-36.1	-34.9

¹ cf. Figure 5

² Surface residual stress predicted in simulation

A comparison of the stress variation by location and process (sample) is plotted in Figure 14.

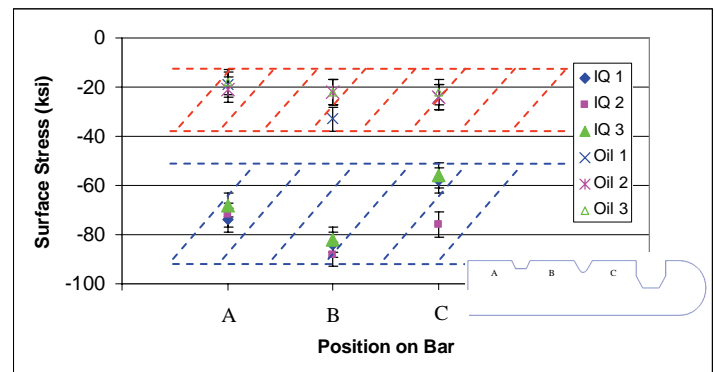


Figure 14: Comparison of Surface Residual Stress Variation at Three Locations on the Notched Specimens

The data show two distinct trends for the six specimens:

1. The intensive quenched specimens show an average increase in surface compression of 50.2 ksi over the corresponding average oil quench results:

Intensive Quench

$$\bar{X} = -74.8 \text{ ksi}$$

$$\sigma = 10.57$$

Oil Quench

$$\bar{X} = -24.6 \text{ ksi}$$

$$\sigma = 3.30$$

2. The 3σ spread (99% variation) for the intensive quench process is +/- 31.7 ksi, vs. +/- 9 ksi for the oil quench.

Given the small sample population, the variance seen in the intensive quench process was strongly influenced by some type of end effect for samples #1 and #3. However, the data provides important indicators to potential fixturing sensitivity for the applied intensive quench practice.

As XRD to determine residual stress is both expensive and time consuming, it is not a practical means of assessing residual stress in a production setting. Consequently an alternative, rapid and nondestructive method using Barkhausen noise (BN) was also investigated for assessing variation in residual stress response. Barkhausen noise is created by changes in a materials magnetization response under an ac magnetizing field.[11] Variations in Barkhausen response are known to be affected by both residual and applied stress. For steels of the same composition and geometry, measuring BN provides a means of gaging residual stress variability. The use of this technique in quality control for critical heat treated steel parts has been increasing. [12]

For this study, a Rollscan300[®] BN unit was calibrated for the Pyrowear 53 material and sample geometry according to published guidelines and standard practice. Using an applied voltage of 4.5V, with a magnetizing frequency of 80 Hz, BN response on surfaces A, B and C (cf. Figure 5) were obtained on each of the six specimens. Figures 15 – 20 show comparative plots of the residual stress calculated from XRD and the measure BN response (magnetic power) at each position for each of the six test coupons. Though not numerically exact, a correlation is clearly evident between the two measurements. The non-destructive Barkhausen noise technique therefore appears to show important potential in production heat treat quality control where a gage of process variability is required. The BN measurements shown in Figures 15 – 20 also provide additional confirmation of the localized process variability seen in the intensively quench coupons.

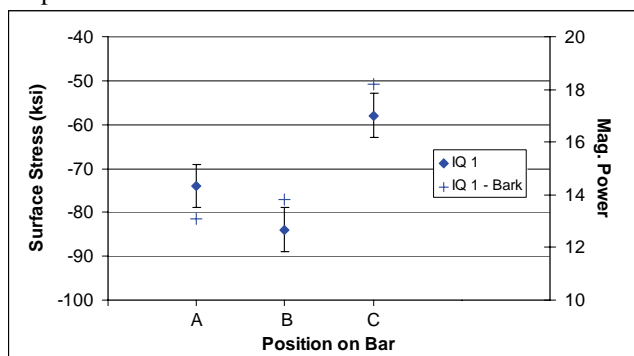


Figure 15: Comparison of Residual Stress Calculated from XRD and BN Measurements by Location on IQ Coupon #1

Heat Treat Simulation

As discussed with the presentation of the distortion and residual stress results, heat treatment computer modeling was used to augment the sensitivity analysis. The model provides key information relating to the sequence of transformation strains relative to thermal gradient changes during the respective heat treatments. It is the variation in this sequence that produces the distortion and residual stress differences, even with nearly identical final hardness and microstructure.

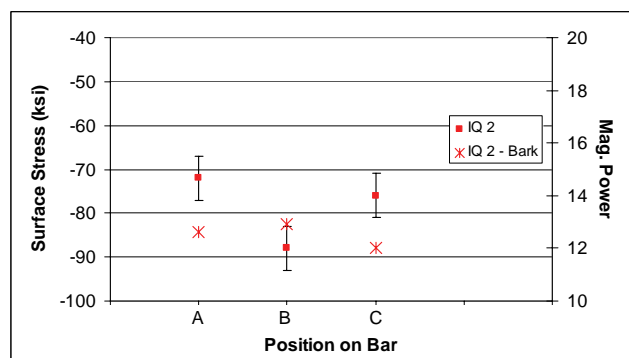


Figure 16: Comparison of Residual Stress Calculated from XRD and BN Measurements by Location on IQ Coupon #2

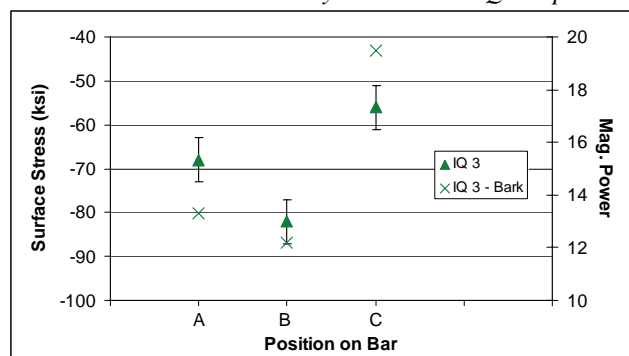


Figure 17: Comparison of Calculated X-Ray and Measured BN Response by Location on IQ Coupon #3

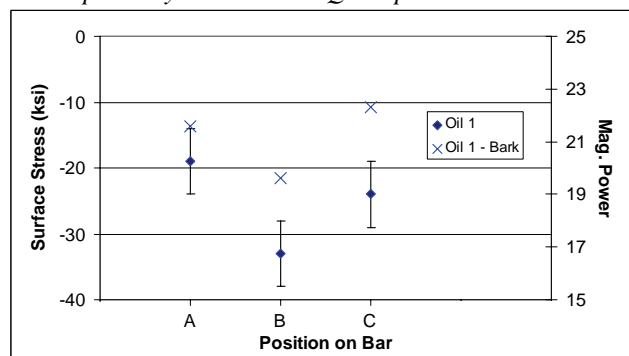


Figure 18: Comparison of Calculated X-Ray and Measured BN Response by Location on OQ Coupon #4

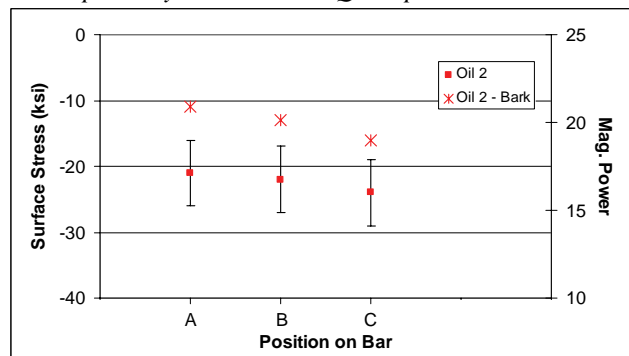


Figure 19: Comparison of Calculated X-Ray and Measured BN Response by Location on OQ Coupon #5

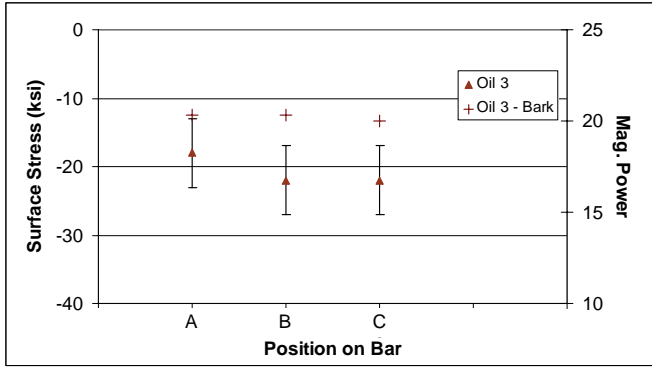


Figure 20: Comparison of Residual Stress Calculated from XRD and BN Measurements by Location on OQ Coupon #6

Figure 21 shows a comparison of the predicted temperature, martensite fraction and residual stress profiles for the two processes at four (4) stages of the heat treatment. From the simulation, one can see the direction of bowing being established early in the quench for both processes. For the oil quench, the martensite transformation in the non-carburized matrix begins at about 5 seconds, with the bulk of the coupon at a temperature range of 380°C - 490°C. For the intensive quenched bar, martensite transformation initiates much earlier (0.5 sec.) with the bar having a gradient of 380°C - 910°C. At 2.5 seconds only the core and carburized surface remain untransformed. The higher thermal gradient permits greater relative shrinking of the hotter core relative to the surface in the intensive quenched coupon, and thus greater retention of the compressive surface stresses at the end of quenching. The transformation of retained austenite during the deep freeze increases the surface residual compression slightly in both cases, with a small corresponding increase in the subsurface tensile stresses.

Tables 5 and 6 provide numeric data from the models for temperature, martensite and stress evolution during quenching and after the deep freeze/double temper. Locations for the data are referenced in Figure 22. Key contrasts between the two practices relating to heat treatment response include:

- 1) For the oil quench, there is virtually no thermal gradient between surface and core when the carburized surface transforms to martensite at ~200 seconds. In the intensive quenched coupon the gradient is 92°C (166°F) when the surface begins transforming at ~5 seconds into the quench.
- 2) In the oil quenched coupon, residual stress remains constant on the non-carburized bottom surface after ~24 seconds into the oil quench, which corresponds to completion of martensite transformation in this region. Part distortion is relatively fixed at this time, changing only after the deep freeze transforms retained austenite at the opposite, carburized surface (cf. Figure 21).

- 3) For intensive quenching, sensitivity is driven primarily by the gradient during quenching. Distortion and residual stress foundations are established principally during the first 5 seconds of quenching.

Table 5: Time, Temperature, Transformation and Residual Stress behavior at 3 Locations in the Notched Coupon during Oil Quenching

OIL QUENCH				
LOC.	TIME (sec)	TEMP °C	MART %	STRESS (ksi)
Carb Surface				
	0	905°C	0	0 ksi
	1	814°C	0	3.1 ksi
	6	414°C	0	-15.3 ksi
	24	179°C	0	39.5 ksi
	215	53°C	75%	-32.7 ksi
	1800	50°C	77%	-32.4 ksi
	Final	20°C	98%	-46.1 ksi
Core				
	0	905°C	0	0 ksi
	1	877°C	0	-9.7 ksi
	6	486°C	0	32.0 ksi
	24	186°C	98%	-60.0 ksi
	215	53°C	99%	-50.8 ksi
	1800	50°C	100%	-50.8 ksi
	Final	20°C	100%	-48.9 ksi
Btm Surf				
	0	905°C	0	0 ksi
	1	814°C	0	4.0 ksi
	6	414°C	72%	-24.7 ksi
	24	179°C	100%	14.1 ksi
	215	53°C	100%	14.1 ksi
	1800	50°C	100%	14.1 ksi
	Final	20°C	100%	11.4 ksi

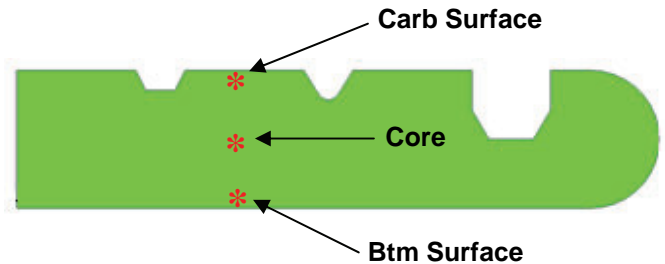
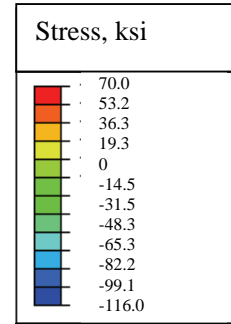
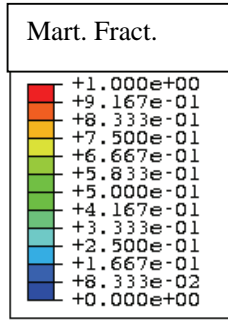
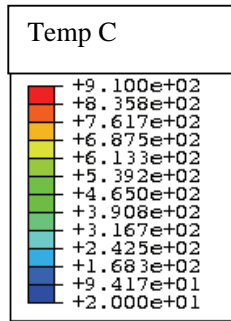


Figure 22: Reference Locations for Quantitative Model Data shown in Tables 5 and 6.



Oil Quench



Time=5 sec



Time=24 sec



Time = 1800 sec (end of quench)



Final



Time=5 sec



Time=24 sec



Time = 1800 sec (end of quench)



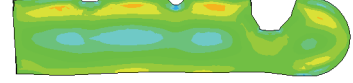
Final



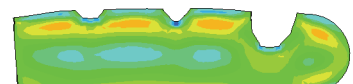
Time=5 sec



Time=24 sec

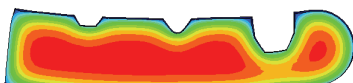


Final

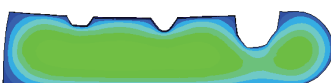


Final

Intensive Quench



Time = 0.5 sec



Time = 2.5 sec



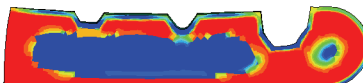
Time = 5 sec (end of quench)



Final



Time = 0.5 sec



Time = 2.5 sec



Time = 5 sec (end of quench)



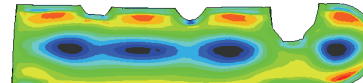
Final



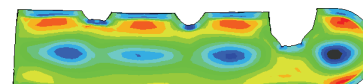
Time = 0.5 sec



Time = 2.5 sec



Time = 5 sec (end of quench)



Final

Figure 21: Time Sequence of Temperature, Martensite Fraction and Axial Stress Profiles predicted by the Computer Model for both Heat Treatment Practices. Coupon Distortion is Magnified 10X.

Table 6: Time, Temperature, Transformation and Residual Stress behavior at 3 Locations in the Notched Coupon during Intensive Quenching

INTENSIVE QUENCH				
LOC.	TIME (sec)	TEMP °C	MART %	STRESS (ksi)
Carb Surface				
	0	905 °C	0	0 ksi
	0.5	405 °C	0	-16.8 ksi
	2.5	216 °C	0	-21.5 ksi
	5.0	84 °C	86%	-50.6 ksi
	Final	20 °C	100%	-84.4 ksi
Core				
	0	905 °C	0	0 ksi
	0.5	872 °C	0	-11.2 ksi
	2.5	505 °C	0	11.5 ksi
	5.0	176 °C	99%	-111.7 ksi
	Final	20 °C	100%	-69.6 ksi
Btm Surface				
	0	905 °C	0	0 ksi
	0.5	430 °C	90%	-32.6 ksi
	2.5	216 °C	99%	-4.5 ksi
	5.0	90 °C	99%	-3.2 ksi
	Final	20 °C	100%	-35.4 ksi

Conclusions

Dimensional and residual stress response during heat treatment can vary significantly based on the sensitivity of a steel part to thermal and transformation strains. Using a simple notched coupon and heat treatment modeling, it is possible to quantify this sensitivity with respect to different heat treatment processes as well as variation within a single heat treating practice.

For Pryowear 53 steel, high hardenability makes use of traditional hardenss and microstructural investigation ineffective as indicators in assessing dimensional change and residual stress differences due to process variation. However, the combined use of a simple notched coupon in combination with heat treat simulation and NDT Barkhausen methods can provide key descriptors of process variation. Such indicators include:

- Part-to-part variability within a given process
- Barkhausen noise variation within a given part indicative of unstable process conditions
- Correlation of thermal/stress simulations with Barkhausen and distortion data, providing “quasi in situ” data on the driving metallurgical mechanisms of the process

Acknowledgements

The authors wish to acknowledge the support of G. Coubrough of Twin Analytical, Ltd. and J. Pineault of Proto Manufacturing Ltd. for their support in distortion measurement and x-ray analysis. Appreciation is also expressed to IQ Technologies in Akron, Ohio for their assistance with heat treatment. Finally, DCT acknowledges the additional support of the US Army AATD for continued recognition of the need for heat treatment sensitivity assessment. Partial support of this work was provided through AATD SBIR project #W911W6-06-C-0062.

References

1. P. Stratton, *Validating the Modeling of a Gas-jet Quenched Carburized Gear*, *Proceedings of the 5th International Conference and European Conference on Heat Treatment*, Assoc., Berlin, Germany 21-30, (2007)
2. Z. Guo, N. Saunders, P. Miodownik, J. Shille, *Modeling Phase Transformations and Material Properties Critical to Prediction of Distortion during Heat Treatment of Steels*, *Proceedings of the 5th International Conference and European Conference on Heat Treatment*, Assoc., Berlin, Germany 183-190, (2007)
3. A. M. Freborg, B. L. Ferguson, Z. Li, D. Schwam and B. J. Smith, *Engineered Heat Treatment for Stronger Aerospace Gears*, *Gear Solutions*, 24-50, July (2006)
4. B. L. Ferguson, A. M. Freborg and Z. Li, *Residual Stress and Heat Treatment – Process Design for Bending Fatigue Strength Improvement of Carburized Aerospace Gears*, *Proceedings of the 5th International Conference and European Conference on Heat Treatment*, Assoc., Berlin, Germany 95-104, (2007)
5. M. Teodorescu, J. Demurger and J. Wendenbaum, *Deformation Forecasting during the Cooling of a Test Part*, *Proceedings of the 23rd Heat Treating Conference*, 203-210, ASM International, Materials Park, Ohio (2005)
6. Z. Li, B. L. Ferguson, X. Sun and P. Bauerle, *Experiment and Simulation of Heat Treatment Results of C-Ring Test Specimen*, *Proceedings of the 23rd Heat Treating Conference*, 245-252, ASM International, Materials Park, Ohio (2005)
7. A. M. Freborg, B. L. Ferguson, Z. Li and D. Schwam, *Bending Fatigue Strength Improvement of Carburized Aerospace Gears*, *Proceedings of the 23rd Heat Treating Conference*, 186-195, ASM International, Materials Park, Ohio (2005)
8. B. L. Ferguson and A. M. Freborg, “Software to Predict Distortion of Heat Treated Components,” *US*

Army SBIR - Phase II Final Report, USAAMCOM TR 02-D-46, (2002).

9. G. Krauss, *Steels: Processing, Structure and Performance*, pp. 417-418, ASM International, Metals Park, Ohio (2005)
10. G. Parrish, *Carburizing: Microstructures and Properties*, pp. 177-195, ASM International, Metals Park, Ohio (1999)
11. K. Titto, *Use of Barkhausen Effect in Testing for Residual Stresses and Material Defects, Residual Stress in Design*, 27-36, ASM International, Materials Park, Ohio (1987)
12. J. Grum, P. Zerovnik and D Fefer, *Use of Barkhausen Effect in Measurement of Residual Stresses in Steel after Heat Treatment and Grinding, Proceedings of the 15th WCNDT Conference, Rome, Italy (2000)*